Using Fluorescence to Characterize the Role of Protein Oligomerization in the Regulation of Gene Expression

Catherine A. Royer

Abstract Gregorio Weber's legacy, in addition to seminal contributions in the application of fluorescence to the study of biological molecules, includes, as well, a profound understanding of how protein–protein interactions are intimately coupled to their interactions with ligands. Such energetic and structural coupling implies that protein sequences have evolved such that these interactions are finely tuned to the physiological habitat and state of the organisms in which these proteins function. The work of my group, in collaboration with a number of biologists and biochemists over the years, has sought to discover how protein–protein interactions, both homologous oligomerization and heterologous complex formation, are implicated in the regulation of gene expression. Herein are given several examples of how fluorescence can be applied to characterize the molecular and energetic basis for the role of protein interactions in the regulation of gene expression. Described are several fluorescence approaches, some quite basic and others more complex, how they were applied to specific gene expression regulatory systems both in vitro and in vivo, and what information could be extracted from the results. Apparent from these few examples is the central role played by protein–protein interactions in these regulatory mechanisms, and how any model for regulatory mechanisms must take into account these higher order protein interactions.

Keywords Allostery • Free energy coupling • Oligomerization • Transcription • Translation

C.A. Royer (✉)
Department of Biological Sciences, Rensselaer Polytechnic Institute, Troy, NY, USA
e-mail: royerc@rpi.edu

D.M. Jameson (ed.), *Perspectives on Fluorescence: A Tribute to Gregorio Weber*,
Springer Ser Fluoresc (2016) 17: 235–254, DOI 10.1007/4243_2016_12,

Contents

1 Introduction

In addition to Gregorio Weber's seminal contributions to the field of biological fluorescence, his work in the area of protein interactions, cooperativity, and allostery remains a major legacy in biochemistry [1]. Given his dual expertise in fluorescence and bio-molecular interactions, it is not surprising that he was able to make great progress in both fields simultaneously. Since Weber's early work on the polarization of fluorescent dyes bound to proteins [2, 3], fluorescence emerged and has remained one of the best methods for quantitative measurements of protein interactions. The widespread use of fluorescence in modern quantitative biology stems from several major advantages over alternative methods, advantages that Gregorio Weber recognized, developed and exploited over his illustrious career. One major advantage of fluorescence is its high sensitivity, which allows for equilibrium measurements of very high affinities between biomolecules. Indeed, with the development of instrumentation capable of single molecule detection, fluorescence has replaced most detection methods based on radioactivity. Another advantage of fluorescence for measuring protein interactions is the fact that binding is determined at equilibrium with no need to separate bound from free species. In addition, given its high sensitivity, fluorescence can be measured very quickly, allowing highly quantitative characterization of the kinetics of protein interactions, extending down to the microsecond range, which is useful for monitoring the intramolecular protein interactions implicated in fast protein folding (e.g., [4, 5]). Fluorescence detection is easily coupled to instrumentation for perturbing equilibria such as stopped flow or titration devices and microfluidic systems, as well as temperature and pressure perturbation. Indeed, Weber pioneered the use of fluorescence coupled to pressure perturbation to monitor protein interactions, both intra- and inter-molecular [6].

Weber used the many fluorescence approaches he developed to probe a number of different types of protein interactions. These include ligand binding (cooperative and antagonistic) [7–14], homologous and heterologous protein subunit interactions [15–25], and the coupling between the two [1, 26]. These studies highlighted the

energetic subtlety of the protein and ligand concentration dependencies of important regulatory circuits. I was a graduate student in Gregorio Weber's group in the early 1980s at the time he was working on the subject of free energy couplings between ligand binding and protein oligomerization. During that period, Brian Matthews visited the University of Illinois and gave a seminar presenting the first 3-D structure of a transcriptional repressor, the *lambda* Cro Repressor dimer [27], which is necessary to induce the lytic cycle of *lambda* phage infection. It binds to two operator regions in the phage DNA in competition with the *cI* repressor, which is required to maintain the lysogenic state. Each of the operator regions contains three binding sites for the repressor dimers, which exhibit different affinities for the different target sites in the operators. Together these two repressors control the switch between lysogenic and lytic phases of infection [28, 29]. Inspired by Brian Matthews' beautiful dimeric structure, the complexity of this apparently finely tuned biological switch and Weber's work on free energy couplings between subunit oligomerization and target binding, I asked if and how protein subunit interactions might be coupled to operator DNA binding in such cases. Indeed, work in the group of Gary Ackers [30–34] and later Don Senear [35, 36] revealed the quantitatively exquisite control at work in *lambda* switch, and the complex oligomerization equilibria involved. In collaboration with Kathleen Matthews we carried out a study of the role of subunit interactions in the mechanism of *lac* repressor function, a major subject of her research group [37–41]. This set me on the path of over thirty years of work using fluorescence approaches to characterize the energetics and structure–function relationships for protein systems implicated in the regulation of gene expression. In this chapter, I will review the major applications of these techniques by my group, highlighting what sort of information they have provided concerning the systems under study.

2 The *Lac* Repressor

I began to work on the *lac* repressor system in collaboration with Kathleen Matthews at Rice University, although less was known from a structural point of view at the time [42, 43] than for the *cI*/*cro* system. The *lac* repressor is predominantly tetrameric. Each monomer is made up of a ligand binding domain, to which the inducer galactose binds in a deep cleft, a linker region and a DNA binding domain. The DNA binding domain forms a helix-turn-helix motif that presents the recognition helix to a half operator site. LacI binds to three operator regions separated by a long intervening loops. Each site can be bound with high affinity by a dimer of the repressor with one DBD interacting in each of two half-sites. High affinity operator interactions are observed for the unliganded protein, and inducer binding (the synthetic inducer iso-propyl-thio-galactoside or IPTG is typically used in vitro) leads to a decrease in affinity for the operator by about five orders of magnitude, depending upon the salt concentration used in the measurements [44].

We used a combination of pressure and tryptophan or dansyl fluorescence polarization and tryptophan emission energy to measure the tetramer–dimer

dissociation and to probe the effect of IPTG binding on this equilibrium [45, 46]. We found that the tetramer–dimer dissociation constant was 14 nM at 21°C and that addition of IPTG stabilized the tetramer against dissociation by a factor of 4 at that temperature. We also found that pressure dissociated the IPTG, with a rather large volume change, ~−70 ml/mol. In addition to revealing a free energy coupling between ligand binding and subunit interactions which could be important in controlling DNA looping upon induction, determination of the affinity between LacI dimers has become somewhat useful in recent years, as the stochastic modeling of transcriptional control by *lac* and other repressors requires knowledge of these constants.

3 The *Trp* Repressor: Affinity and Cooperativity

I became interested in another bacterial transcription factor, the *trp* repressor (TrpR), because its function was more akin to a rheostat than the toggle switch of the *lac* repressor. *Trp* repressor represses transcription of genes in *E. coli* involved in the biosynthesis of tryptophan [47–49]. It also represses its own transcription [50]. Its affinity for the three (*trp*, *aroh*, and *trpR*) operator sites is controlled by the co-repressor, tryptophan, such that when tryptophan is plentiful, it binds to TrpR, increasing its affinity for the operator sites and shutting down transcription of the tryptophan biosynthesis genes. However, since it also shuts down its own transcription at the *trpR* site, this decreases gradually the repressor concentration, leading to a gradual relief of repression that is accentuated if, in addition, tryptophan levels drop.

Typically at that time, protein–DNA interaction affinities were measured using either nitrocellulose filter binding assays or electrophoretic mobility shift assays (EMSA), both relying on radiolabeled oligonucleotides. Neither of these techniques is an equilibrium technique, since they involve separation of the free from bound species. Moreover, it is difficult to implement studies of the effects of solution conditions or temperature because the conditions for the function of the assays themselves are rather stringent. Trained by Gregorio, it occurred to me that a fluorescence anisotropy-based assay would provide an attractive alternative to these techniques. The sensitivity could be nearly as good as the radioactive assays and the measurement is made in solution at equilibrium, with no need to separate the bound from the free species. In previous studies by us and others using dyes of rather low quantum yield and wavelength, high affinity interactions could not be measured [51–53]. To overcome this limitation, we chose to use an oligonucleotide labeled at the 5′ end via phosphoramidite chemistry with fluorescein via a six carbon linker. We chose fluorescein as a dye because it was the most sensitive at the time. At neutral pH, the quantum yield was sufficiently high and the wavelength sufficiently removed from UV contaminants, that we could detect quite well, with some modifications to the instrument, 200 pM concentrations of fluorescein. At the time it had become possible to purchase custom labeled oligonucleotides from Promega Corporation (Madison, WI), as such labeling was being explored for use

in new fluorescence-based sequencing approaches that are the norm today. Using a solution containing 200 pM of this 5′ fluorescein labeled double-stranded 25mer oligonucleotide containing the sequence of the trp operator, also in collaboration with Kathleen Matthews, we carried out measurements of protein–DNA interactions based on anisotropy [54]. We found that TrpR bound to its operator cooperatively, and analyzed the binding with a model of coupled monomer–dimer and dimer DNA binding, which yielded dissociation constants of 4 and 0.1 nM, respectively. We were also able to directly measure the effect of tryptophan on the interaction (Fig. 1).

The thermodynamic binding model used to fit the data in Fig. 1 was based on the crystal structure of the *trp* repressor bound to a target oligonucleotide, the first repressor-operator co-complex ever published [55]. It revealed a dimer of the repressor with the recognition helix of the helix-turn-helix motif interacting with at CTAG palindromic sequence. However, the actual stoichiometry of binding and the true recognition sequence came into question. Uncertainty concerning stoichiometry and target sequence is rather typical in the case of protein–DNA interactions. Using a variety of techniques, fluorescence anisotropy, but also analytical ultracentrifugation, we and our collaborators had demonstrated that the repressor itself, in solution formed higher order oligomers that could be disrupted by the addition of the co-repressor, tryptophan or salt [51, 56]. Jannette Carey and colleagues published a crystal structure of an oligomeric form of *trp* repressor bound to a target sequence in which an alternative recognition mode was evident via a GNACT palindrome [57]. We went on to use fluorescence anisotropy, fitting the high affinity binding event as a cooperative dimer–tetramer equilibrium and demonstrated that the stoichiometry and affinity of the *trp* repressor-operator interactions depended on the length and sequence of the target oligonucleotide, with the different natural targets exhibiting different stoichiometry and cooperativity [58, 59].

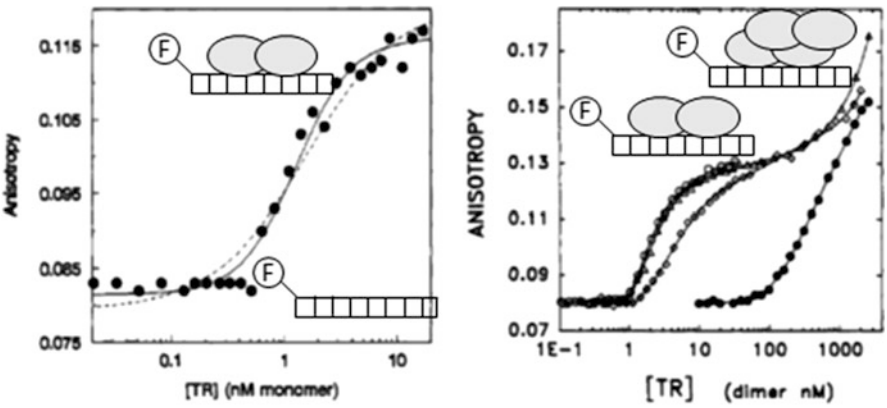

Fig. 1 Anisotropy titration of 5′ fluorescein labeled 25mer oligonucleotide bearing the trp operator sequence at 21°C pH 7.6 10 mM phosphate buffer with purified trp repressor. (*Left*) 300 pM 25mer; (*Right*) 30 nM 25mer with 0 (*closed circles*), 0.04 (*open diamonds*), 0.4 (*open triangles*), and 4.0 (*open circles*) mM L-tryptophan. Figures reworked from [54]

We also examined the effect of super-repressor mutations on DNA binding [60]. Using a variety of fluorescence techniques and isothermal titration calorimetry we demonstrated that the super-repressor phenotype of the AV77 super-repressor discovered by Yanofsky and coworkers [61] was due to the fact that the free WT protein is partially unfolded in the DNA binding domain and that substitution of alanine by valine at the N-cap position of the recognition helix stabilized it in its folded form such that the binding of tryptophan, which also stabilizes the recognition helix, had little further effect in the super-repressor mutant [62]. It has recently come to my attention (Harish Subramanian and Jannette Carey, personal communication) that the TrpR DBD is not unfolded in absence of tryptophan, but in equilibrium between multiple conformations. In addition to a large number of studies by the Yanofsky, Carey, Sigler, Hurlburt, Matthews, Jardetsky, and other groups that will not be covered here, this ensemble of fluorescence studies on a transcriptional regulator, augmented by crystallography, calorimetry, analytical ultracentrifugation, and circular dichroism, allowed a highly quantitative and thorough characterization of the molecular mechanisms and thermodynamics in this highly complex regulatory system involving coupled folding, oligomerization, ligand binding, and DNA target recognition, all exquisitely tuned to achieve the appropriate level of tryptophan synthesis and energy usage for *E. coli* under varying nutrient conditions.

4 Nuclear Receptor Ligand Modulated Heterologous Protein Interactions

Nuclear receptors (NR) comprise a large family of ligand modulated transcription factors responsible for many important aspects of differentiation, growth, and homeostasis in metazoans [63]. There are two major subfamilies of NRs, the homo-dimeric NRs, which include the hormone receptors, estrogen receptors (ER), glucocorticoid receptors (GR), and androgen receptors (AR), and which bind to palindromic DNA target sites and the hetero-dimeric NRs, such as the retinoid receptors, RXR/RAR, thyroid hormone receptors, TR, peroxisome proliferator receptors, PPARs, etc., which bind to direct repeats. The NRs harbor structurally homologous C-terminal ligand binding domains, generally endowed with a ligand-dependent activation domain in the C-terminal helix, a DNA binding domain, and a highly variable N-terminal domain that can also exhibit activation functions. NRs interact with ligands (agonists, antagonists, partial agonists, and inverse agonists), which are generally hydrophobic in nature, although some NRs are thought to respond to gases such as NO via a bound heme moiety. Ligand binding modulates NR interactions with co-repressors and coactivators of transcription, which themselves exhibit chromatin remodeling activity and recruit other transcription factors. The stoichiometries, affinities, and cooperativity of the multiple linked interactions implicated in NR function are finely tuned to the proper level of control of these important physiological functions. Indeed, NRs represent

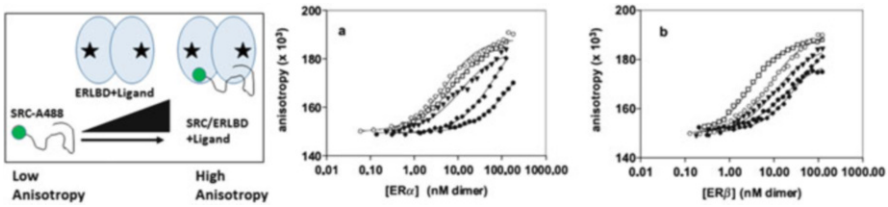

Fig. 2 Titrations of 2 nM Alexa488 labeled 26 kDa fragment of the SRC-1 NR coactivator with either ERα or ERβ in presence of saturating concentrations of agonist ligands, estradiol (*open circles*), genistein (*open squares*), estrone (*closed circles*), estriol (*triangles*), and ethylene estradiol (*diamonds*)

an important class of targets for development of therapeutic agents, many of which have long been on the market, for the treatment of human disease states including many forms of cancer, heart disease, diabetes, and inflammation. Not surprisingly, the literature on NR structure function relationships is vast, and will not be reviewed here. However, few groups have been interested in deciphering the complex energetic relationships between ligand binding, both homologous and heterologous protein interactions and nucleic acid interactions. One exception is the work of David Bain's group [64, 65]. For our part, often in collaboration with the structural group of William Bourguet, we have used fluorescence anisotropy to investigate ligand-dependent NR-DNA interactions [66–69] and NR-coregulator interactions [70–75].

We were the first to use anisotropy to investigate the impact of different types of ligands on NR interactions with fluorescently labeled peptides derived from co-activators (Fig. 2) [73]. We found differential effects of ligands for recruitment of the SRC-1 coactivator to two different subtypes of ER. Such differences can have significant impact on tissue specific therapeutic effects, since the ER subtypes are differentially expressed in different tissues. Indeed, this anisotropy assay for the effect of ligands on NR coregulator interactions has become a common practice in the pharmaceutical industries drug development programs targeting NRs. Following Schwabe and co-workers [76], we also used C-terminal labeling of the activation helix 12 on RAR to investigate by time-resolved anisotropy, the effects of ligation and peptide binding on the dynamics of this all important helix [71]. More recently, we have used FCS to measure the ER-Tif2 coactivator interaction K_d as a function of ligand in live Cos7 cells, using transient transfection of cerulean and mCherry fusions of the two proteins [77].

5 Translational Control of Ribosomal Protein Production: L20 – Stoichiometry

As noted above, ascertaining the stoichiometry of protein–nucleic acid complexes under physiologically significant conditions of concentration, temperature, salt, etc., is often rather challenging. A lack of clarity as to the stoichiometry of the

large ribosomal protein, L20, from *E. coli* and other bacterial species with a long and complex translational operator on its messenger RNA illustrates the issue [78–82]. The translational operator RNA sequence comprises hundreds of base pairs and forms a required long-range pseudoknot that is recognized by L20 and which overlaps the Shine-Dalgarno sequence of the mRNA. Another similar site also exists within this operator, and both sites mimic the site recognized by L20 in the 16S ribosomal RNA. Both sites are required for translational control in vivo. Anisotropy assays had indicated that perhaps the stoichiometry might not be 2:1, at least under the conditions of titrations. In this case we used fluorescence correlation spectroscopy (FCS) and fluorescence cross-correlation spectroscopy (FCCS), to ascertain whether two molecules of L20 could bind to the operator RNA. FCS first proposed by Magde et al. [83] uses the fluctuations in fluorescence intensity in a small confocal observation (or in our case 2-photon excitation) volume to characterize the concentration and diffusion properties of the molecules. If one uses molecules labeled with different colors in two different detection channels it is possible to deduce whether the two molecules form a complex. For a review of FCS and FCCS, see [84].

We labeled separately two solutions of a C-terminal construct of L20 known to be sufficient for translational control in vivo, with a green and red fluorescent dye (Alexa 488 and Atto647N) on the N-terminus of the protein via succinimidyl ester chemistry. First, we carried out FCS experiments observing only the fluorescence from the Alexa488 (green) labeled L20 (Fig. 3, left). Upon addition of the operator RNA at a concentration tenfold the K_d [85] determined by anisotropy, the correlation profile shifted to longer lag times, indicating binding of the protein to the RNA (which was large, 660 base pairs). Then, still observing in the green channel, we added the red (Atto647N) labeled L20. If two or more molecules of L20 could bind to the RNA, then we would have expected (under the equimolar conditions used) that the curve would remain at the same lag time, since the L20 C-terminal

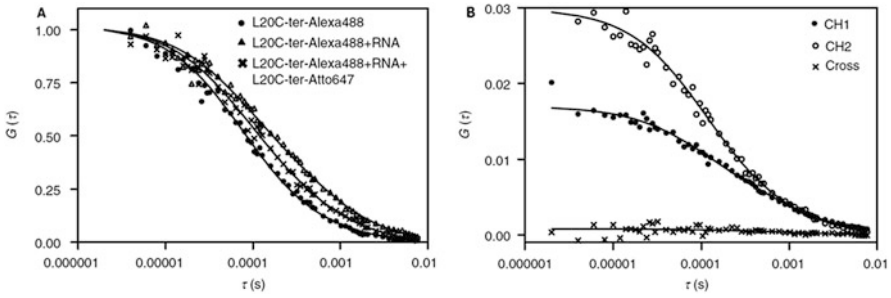

Fig. 3 Stoichiometry of the L20-operator RNA complex investigated by fluorescence correlation spectroscopy. (*Left*) 150 nM L20-Alexa488 (*circles*), plus 150 nM operator RNA (*triangles*), and 150 nM L20-Alexa488, plus 150 nM operator RNA, plus 150 nM L20-Atto647N (*crosses*); (*Right*) 150 nM L20-Alexa488, plus 150 nM operator RNA plus 150 nM L20-Atto647N – Alexa488 channel (*closed circles*), Atto647N channel (*open circles*), cross-correlation (*crosses*). Figures reworked from [85]

construct is only 6 kDa, and would not be expected to make a significant difference to the diffusion time of the already large complex of the operator RNA bound by the green labeled L20. Instead, the curve was shifted back to faster diffusion times, indicating that the green L20 was competed off of the operator RNA by the red L20. To further demonstrate that two L20 proteins could not bind simultaneously to the operator RNA, we carried out cross-correlation measurements. Here we added equimolar amounts of L20 green and L20 red, with the RNA at a concentration tenfold above the K_d [85]. If more than one L20 molecule could interact simultaneously with the RNA, then we would have expected to see some cross-correlation signal. Instead, absolutely no cross-correlation amplitude was observed (Fig. 3, right), indicating that the stoichiometry of the L20/operator RNA complex was 1:1, despite the existence of two possible sites. Further studies indicated anti-cooperative allosteric interaction between the two putative binding sites on the operator RNA [85].

6 Control of the Switch Between Glycolysis and Gluconeogenesis in *B. subtilis*

In collaboration with Nathalie Declerck and Stephane Aymerich, we set out to use fluorescence approaches in the characterization of the molecular mechanisms of transcriptional regulators involved in the control of the central carbon metabolism in the soil bacterium, *Bacillus subtilis*. The switch between glycolysis and gluconeogenesis in *B. subtilis* is controlled at the level of the transformation of glyceraldehyde phosphate to 1,3-diphosphoglycerate (Fig. 4) [86–88]. The reaction in the glycolysis direction is catalyzed by the GapA enzyme, while the reverse reaction, unlike in *E. coli*, requires a second enzyme, GapB. Expression of GapA is controlled at the transcriptional level by the central glycolytic genes repressor or CggR. CggR is induced by fructose bis-phosphate (FBP) a product of glucose degradation. Expression of the GapB enzyme is very strongly catabolite repressed when cells are grown on a glycolytic carbon source by the control catabolite protein of gluconeogenic genes (CcpN). The mode of induction of CcpN upon a nutrient shift to gluconeogenic carbon sources, such as malate, is not known, but genetic evidence suggests that the co-transcribed YqfL protein is implicated [88].

6.1 In Vitro Biophysical Studies

The groups of Declerck and Aymerich had investigated in detail the structural and in vivo functional properties of this genetic metabolic switch. Our collaboration with these groups involved applying a variety of fluorescence approaches, coupled with other biophysical methodologies, to characterize the energetic couplings

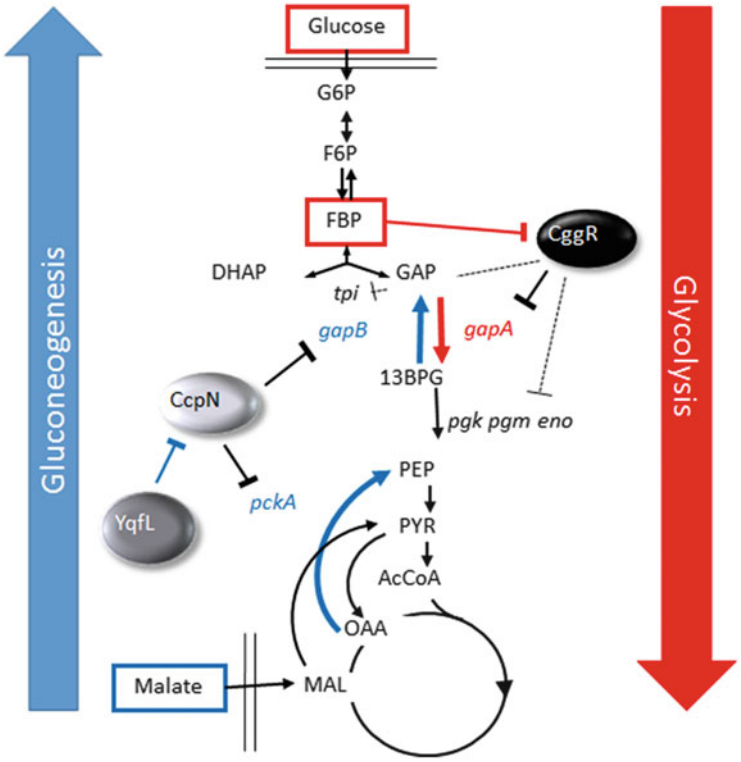

Fig. 4 Schematic diagram of the switch between glycolysis and gluconeogenesis in *B. subtilis*. In *blue*, operative interactions under gluconeogenesis and in *red* operative interactions under glycolysis. Repressor proteins and co-regulators are shown as *black* and *grey* ellipses

implicated in their function. In the case of CcpN, the repressor that strongly downregulates the *gapB* and *pckA* promoters on glucose, we showed by FCCS, using DNA oligonucleotides labeled with a red dye and the CcpN protein labeled with a green dye (Fig. 5) that the stoichiometry of binding was different on oligonucleotides bearing the proposed sequence recognition motifs for these two operator sites [89]. Plotting the ratio of the cross-correlation amplitude to that of the amplitude of the fluctuations in the green channel (that of the protein, tenfold more concentrated than the red-labeled target DNA oligonucleotides) provides a direct measure of binding, and the value of this ratio at the plateau of the binding curve depends upon the stoichiometry of the complex. Indeed it can be seen directly from the Go_x/Go_G ratios in Fig. 5, that the stoichiometry of one complex is approximately twice that of the other. Correcting for labeling ratios and CcpN oligomerization, we deduced stoichiometries of dimer and tetramer, respectively, for the *gapB* and *pckA* target oligonucleotides. Later it was shown that the target sequence for the *gapB* oligonucleotide was not complete, and that the protein bound as a tetramer to the full-length *gapB* target as well.

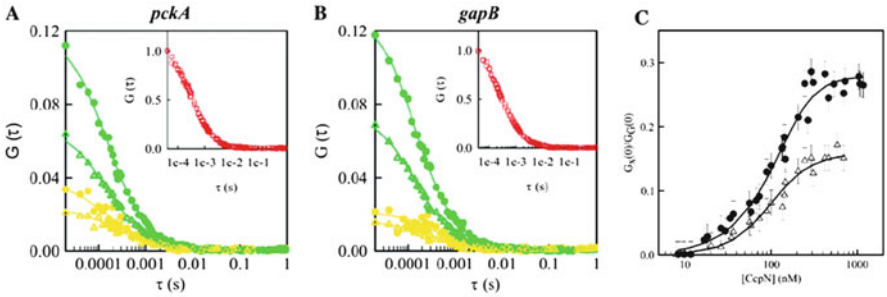

Fig. 5 FCCS measurements of CcpN interaction with target oligonucleotides bearing recognitions sequences for the operators present in the *pckA* and *gapB* promoters. *Red curves* are the FCS profiles for the oligonucleotides labeled with the red dye, Atto-647N. *Green curves* are the FCS profiles for the CcpN protein labeled with fluorescein. The FCCS (cross-correlation) profiles are shown in *yellow*. (**a**) CcpN interactions with the *pckA* oligonucleotide. (**b**) CcpN interactions with the *gapB* oligonucleotide. (**c**) Go_x/Go_G ratio for the pckA and gapB targets as a function of CcpN concentration

Co-variance analysis was used in the case of the CggR protein to investigate the coupled effects of ligand binding and oligomerization in the control of its operator interactions. CggR represses transcription of the *gapA* operon when the bacteria are grown on gluconeogenic carbon sources, such as malate (see schematic in Fig. 4). In addition to the genes coding for the glycolytic enzymes, the first gene in the *gapA* operon is that encoding CggR itself, such that this system includes an autorepression loop. CggR is induced (i.e., dissociates from the operator) when the bacteria sense glucose in the environment. It had been thought that the inducer was FBP. Our work using fluorescence and other biophysical approaches confirmed this hypothesis and demonstrated that FBP played a structural role as well, with two binding sites per CggR monomer. The high affinity site was the structural stabilization site, while the low affinity site was responsible for allosteric induction of CggR [90]. In a classical Weber free energy coupling analogy, using fluorescence anisotropy and analytical ultracentrifugation, we showed how inducer binding was allosterically coupled to cooperative DNA binding by CggR [91].

A model based on these data by which FBP binding leads to CggR tetramer dissociation, and hence decreased affinity and cooperativity in operator binding was confirmed using a combination of FCCS, non-covalent mass spectrometry, and small angle X-ray scattering [92]. The effect of FBP on dimerization is most clearly shown in the FCCS profiles in Fig. 6. Two double-stranded DNA oligonucleotides containing CggR half-sites (able to bind one CggR dimer) were labeled with a red and a green dye, respectively, on the 5′-end of the sense and anti-sense strand. When annealed with their complementary unlabeled strand and mixed in absence of CggR, no interaction between the two double-stranded oligonucleotides is observed, as expected (Fig. 6a). When the two labeled complementary oligonucleotides are annealed, cross-correlation is observed (Fig. 6b). The cross-correlation amplitude is not 100% due to imperfect labeling ratios of the oligonucleotides. If

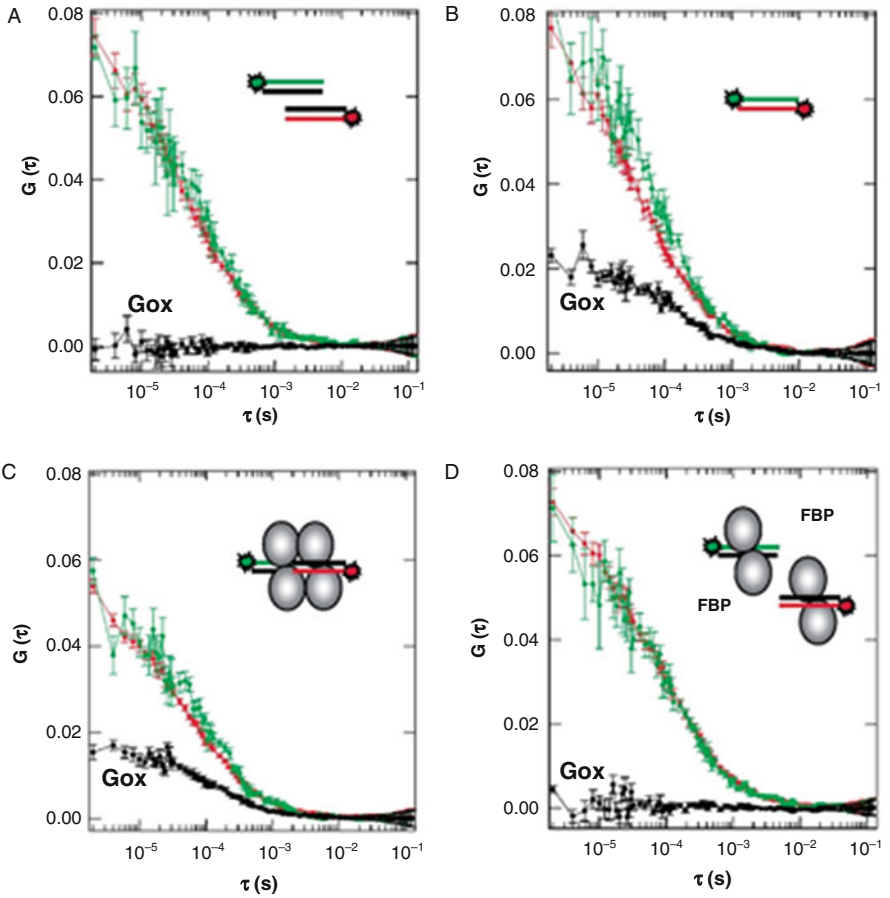

Fig. 6 FCCS measurements of CggR interaction with target oligonucleotides bearing recognitions sequences for half-site operators. (**a**) Two singly labeled double-stranded oligonucleotides labeled, respectively, on the 5′-end of the sense strand for one with fluorescein and the 5′-end of the anti-sense strand for the other with Atto 647N. *Green* and *red curves* are FCS profiles for the *red* and *green* labeled oligonucleotides as depicted in the schematics. *Black curves* are cross-correlation profiles between the *red* and the *green* detected fluorescence. CggR protein is depicted as *grey* ellipses. (**a**) 60 nM each of separately labeled *green* and *red* double-stranded oligonucleotides with the CggR half-sites. (**b**) 60 nM doubly labeled double-stranded oligonucleotide with the CggR half-site. (**c**) 60 nM each of the two separately labeled double-stranded oligonucleotides in presence of saturating CggR protein. (**d**) 60 nM each of the two separately labeled double-stranded oligonucleotides in presence of saturating CggR protein (300 nM in monomer units) and 0.5 mM FBP

the two separately labeled double-stranded oligonucleotides are mixed with the CggR protein in absence of FBP, cross-correlation is observed (Fig. 6c), and the amplitude under these concentrations conditions is maximal, with respect to that observed for the doubly labeled double-stranded oligonucleotide in Fig. 6b. This

indicates that the CggR tetramer can non-covalently cross-link the two oligonucleotides into a single complex. However, this interaction is abolished when FBP is added (Fig. 6d), although mass spectrometry and fluorescence anisotropy demonstrated that the protein is still bound to DNA under these conditions. However, the CggR is dimeric in presence of FBP and can no longer cross-link the two oligonucleotides.

6.2 *In Vivo Fluctuation Microscopy*

The above in vitro biophysical studies on the CcpN/CggR control of the switch between glycolysis and gluconeogenesis provided models for how the proteins functioned in vivo. In the case of the CcpN protein, we hypothesized a "hold back" mechanism, by which the CcpN protein bound to the operator overlapping the *gapB* and *pckA* promoters, would interact directly with the RNA polymerase, preventing transcription initiation. In the case of the CggR repressor a "road-block" model proposed that CggR bound to the operator, downstream of the start site of the *gapA* promoter and blocked transcription elongation by RNA polymerase. We sought to verify these proposed models in vivo using an advanced microscopy technique based on fluorescence fluctuations introduced by Digman and Gratton in 2008 and called scanning Number and Brightness [93]. In scanning Number and Brightness, two-photon in our case, a field of view is imaged using rapid scanning of the excitation laser via galvanometric mirrors, such that the dwell-time at each pixel is shorter than the diffusion time (i.e., that one is sampling at a rate near the top of the FCS curves shown in Figs. 5 and 6, for example). Multiple (50–100) raster scans of the field of view (FOV) are carried out, such that at each pixel, one has 50–100 values for the fluorescence intensity. If the fluorescent molecules have diffused in the time between imaging of the same pixel (about 2–3 s for the frame time), then the fluorescence intensity values incorporate fluctuations due to diffusion. The average and variance of these values at each pixel can be used in a moment analysis to calculate the number of fluorescent molecules in the excitation volume at each pixel, and their molecular brightness. These values must be corrected for shot noise and where possible background auto-fluorescence contributions.

We adapted the two-photon scanning N&B approach to determine the level of gene expression from bacterial GFP promoter fusions [94]. Given the low photon statistics and small size of the bacteria, pixel averaging strategies were implemented in order to obtain robust values for single cell GFP concentrations. We then used this approach to measure and model stochastic expression form the *gapA* and *gapB* GFP promoter fusions in the natural chromosomal locus of *B. subtilis* grown on glycolytic (glucose) and gluconeogenic (malate) carbon sources (Fig. 7). This approach, which yields absolute protein concentrations for single cells, allows for stochastic modeling and absolute determination of the biological noise parameters (Fig. 8). Extremely strong catabolite repression with low noise for the CcpN repressor, and high noise repression for CggR support the

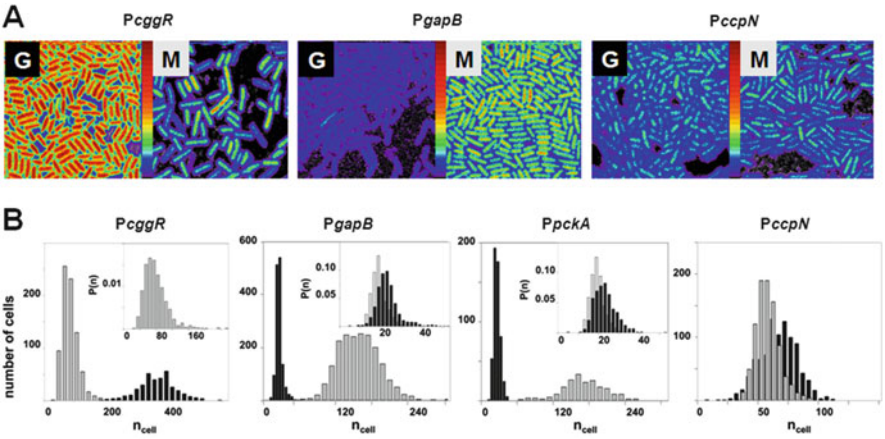

Fig. 7 Scanning 2-photon N&B measurements on *B. subtilis* live cells expressing GFP from promoter fusions of the *gapA*, *gapB*, *pckA*, and *pccpN* promoters. (**a**) Images of bacteria on pads in presence of G, glucose or M, malate for the *gapA*, *gapB*, and *pccpN* promoters as labeled. (**b**) Histograms of the number of GFP molecules in the excitation volume from the quantification of multiple FOV for the *gapA*, *gapB*, *pckA*, and *pccpN* promoters in presence of glucose (*black*) or malate (*grey*)

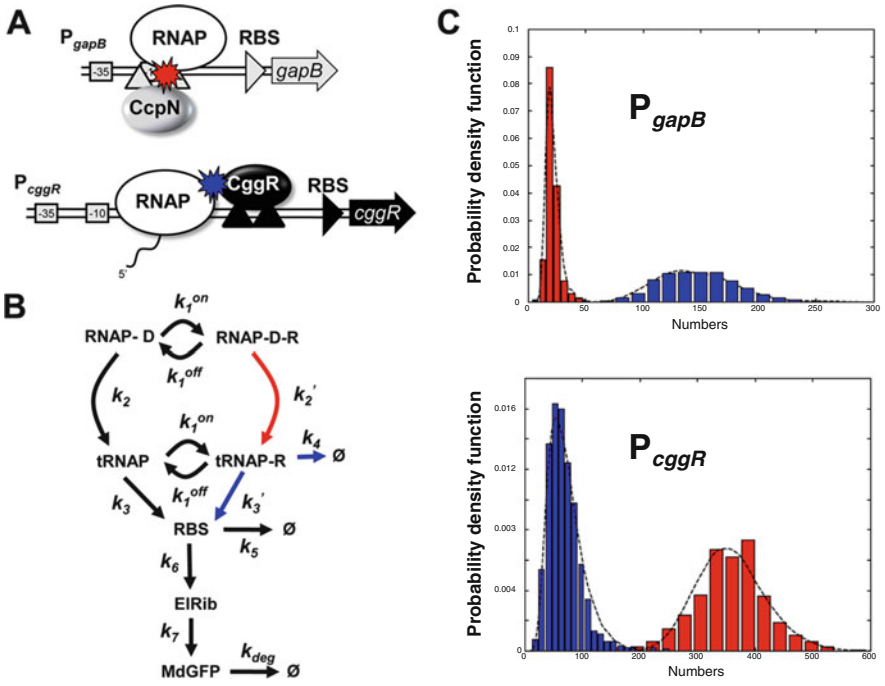

Fig. 8 Stochastic modeling based on the scanning 2-photon N&B measurements on *B. subtilis* live cells expressing GFP from promoter fusions of the *gapA*, *gapB*, *pckA*, and *pccpN* promoters. (**a**) The "hold back" and "road block" models for CcpN and CggR repression, respectively. (**b**) Stochastic model for repression. (**c**) Fits of the experimental distributions for GFP expression on glucose (*red*) and malate (*blue*) to the model in (**b**) for *pccpN* and *pcggR* promoters as labeled

"hold back" and "road block" mechanisms for CcpN and CggR, respectively. Stochastic modeling of the gapA/gapB promoter system under different nutrients yielded rate constants that were entirely consistent with the biophysical models.

7 Conclusions

The above set of examples serves to illustrate how multiple fluorescence approaches can be used both in vitro and in vivo to reveal the very subtle mechanisms underlying the regulation of gene expression. These examples are by no means exhaustive, and our group as well as many others has applied such approaches to multiple protein systems involved in gene regulation. What is clear from these examples is the central role of protein oligomerization interactions, both homologous and heterologous, in the fine tuning of gene expression levels. This key role of protein interactions is a lesson learned from Gregorio Weber, whose insight continues to inspire all of the work of my group. Protein stoichiometry is often missing in the models proposed for biological regulation of gene expression, as well as many other important physiological processes. The work we have carried out over the years, some of which is presented here, underscores that quantitative determination of the coupling between protein–protein interactions and transcriptional regulation is absolutely required for the understanding of these systems, and eventually, the intelligent modulation of their activity in the context of therapeutic strategies to combat disease.

References

1. Weber G (1972) Ligand binding and internal equilibria in proteins. Biochemistry 11:864–878
2. Weber G (1952) Polarization of the fluorescence of macromolecules. I. Theory and experimental method. Biochem J 51:145–155
3. Weber G (1952) Polarization of the fluorescence of macromolecules. II. Fluorescent conjugates of ovalbumin and bovine serum albumin. Biochem J 51:155–167
4. Dumont C, Emilsson T, Gruebele M (2009) Reaching the protein folding speed limit with large, sub-microsecond pressure jumps. Nat Methods 6:515–519
5. Zhu L, Ghosh K, King M, Cellmer T, Bakajin O, Lapidus LJ (2011) Evidence of multiple folding pathways for the villin headpiece subdomain. J Phys Chem B 115:12632–12637
6. Weber G, Drickamer HG (1983) The effect of high pressure upon proteins and other biomolecules. Q Rev Biophys 16:89–112
7. Anderson SR, Weber G (1969) Fluorescence polarization of the complexes of 1-anilino-8-naphthalenesulfonate with bovine serum albumin. Evidence for preferential orientation of the ligand. Biochemistry 8:371–377
8. Weber G (1974) Addition of chemical and osmotic energies by ligand-protein interactions. Ann N Y Acad Sci 227:486–496
9. Weber G (1972) Addition of chemical and osmotic free energies through negative interaction of protein-bound ligands. Proc Natl Acad Sci U S A 69:3000–3003
10. Weber G (1982) Asymmetric ligand binding by haemoglobin. Nature 300:603–607

11. Daniel E, Weber G (1966) Cooperative effects in binding by bovine serum albumin. I. The binding of 1-anilino-8-naphthalenesulfonate. Fluorimetric titrations. Biochemistry 5:1893–1900
12. Weber G, Daniel E (1966) Cooperative effects in binding by bovine serum albumin. II. The binding of 1-anilino-8-naphthalenesulfonate. Polarization of the ligand fluorescence and quenching of the protein fluorescence. Biochemistry 5:1900–1907
13. Kolb DA, Weber G (1975) Cooperativity of binding of anilinonaphthalene sulfonate to serum albumin induced by a second ligand. Biochemistry 14:4476–4481
14. Weber G (1975) Energetics of ligand binding to proteins. Adv Protein Chem 29:1–83
15. Brewer JM, Weber G (1968) The reversible dissociation of yeast enolase. Proc Natl Acad Sci U S A 59:216–223
16. Erijman L, Weber G (1991) Oligomeric protein associations: transition from stochastic to deterministic equilibrium. Biochemistry 30:1595–1599
17. Erijman L, Lorimer GH, Weber G (1993) Reversible dissociation and conformational stability of dimeric ribulose bisphosphate carboxylase. Biochemistry 32:5187–5195
18. Foguel D, Weber G (1995) Pressure-induced dissociation and denaturation of allophycocyanin at subzero temperatures. J Biol Chem 270:28759–28766
19. King L, Weber G (1986) Conformational drift of dissociated lactate dehydrogenases. Biochemistry 25:3632–3637
20. Paladini AA Jr, Weber G (1981) Pressure-induced reversible dissociation of enolase. Biochemistry 20:2587–2593
21. Pin S, Royer CA, Gratton E, Alpert B, Weber G (1990) Subunit interactions in hemoglobin probed by fluorescence and high-pressure techniques. Biochemistry 29:9194–9202
22. Rawitch AB, Weber G (1972) The reversible association of lysozyme and thyroglobulin. Cooperative binding by near-neighbor interactions. J Biol Chem 247:680–685
23. Ruan K, Weber G (1988) Dissociation of yeast hexokinase by hydrostatic pressure. Biochemistry 27:3295–3301
24. Silva JL, Miles EW, Weber G (1986) Pressure dissociation and conformational drift of the beta dimer of tryptophan synthase. Biochemistry 25:5780–5786
25. Xu G, Weber G (1982) Dynamics and time-averaged chemical potential of proteins: importance in oligomer association. Proc Natl Acad Sci U S A 79:5268–5271
26. Weber G (1984) Order of free energy couplings between ligand binding and protein subunit association in hemoglobin. Proc Natl Acad Sci U S A 81:7098–7102
27. Anderson WF, Ohlendorf DH, Takeda Y, Matthews BW (1981) Structure of the cro repressor from bacteriophage lambda and its interaction with DNA. Nature 290:754–758
28. Reichardt LF (1975) Control of bacteriophage lambda repressor synthesis after phage infection: the role of the N, cII, cIII and cro products. J Mol Biol 93:267–288
29. Reichardt LF (1975) Control of bacteriophage lambda repressor synthesis: regulation of the maintenance pathway of the cro and cI products. J Mol Biol 93:289–309
30. Ackers GK, Johnson AD, Shea MA (1982) Quantitative model for gene regulation by lambda phage repressor. Proc Natl Acad Sci U S A 79:1129–1133
31. Darling PJ, Holt JM, Ackers GK (2000) Coupled energetics of lambda cro repressor self-assembly and site-specific DNA operator binding I: analysis of cro dimerization from nanomolar to micromolar concentrations. Biochemistry 39:11500–11507
32. Darling PJ, Holt JM, Ackers GK (2000) Coupled energetics of lambda cro repressor self-assembly and site-specific DNA operator binding II: cooperative interactions of cro dimers. J Mol Biol 302:625–638
33. Johnson AD, Poteete AR, Lauer G, Sauer RT, Ackers GK, Ptashne M (1981) Lambda repressor and cro—components of an efficient molecular switch. Nature 294:217–223
34. Shea MA, Ackers GK (1985) The OR control system of bacteriophage lambda. A physical-chemical model for gene regulation. J Mol Biol 181:211–230

35. Senear DF, Laue TM, Ross JB, Waxman E, Eaton S, Rusinova E (1993) The primary self-assembly reaction of bacteriophage lambda cI repressor dimers is to octamer. Biochemistry 32:6179–6189
36. Senear DF, Ross JB, Laue TM (1998) Analysis of protein and DNA-mediated contributions to cooperative assembly of protein-DNA complexes. Methods 16:3–20
37. Dunaway M, Manly SP, Matthews KS (1980) Model for lactose repressor protein and its interaction with ligands. Proc Natl Acad Sci U S A 77:7181–7185
38. Dunaway M, Matthews KS (1980) Hybrid tetramers of native and core lactose repressor protein. Assessment of operator and nonspecific DNA binding parameters and their relationship. J Biol Chem 255:10120–10127
39. Dunaway M, Olson JS, Rosenberg JM, Kallai OB, Dickerson RE, Matthews KS (1980) Kinetic studies of inducer binding to lac repressor.operator complex. J Biol Chem 255:10115–10119
40. Friedman BE, Olson JS, Matthews KS (1977) Interaction of lac repressor with inducer, kinetic and equilibrium measurements. J Mol Biol 111:27–39
41. Swint-Kruse L, Matthews KS (2009) Allostery in the LacI/GalR family: variations on a theme. Curr Opin Microbiol 12:129–137
42. Matthews HR, Thielmann HW, Matthews KS, Jardetzky O (1973) NMR studies of the binding of an inducer and an anti-inducer to the lac repressor. Ann N Y Acad Sci 222:226–229
43. Matthews KS, Wade-Jardetzky NG, Graber M, Conover WW, Jardetzky O (1977) High resolution 1H NMR of a selectively deuterated analogs of the lac repressor. Biochim Biophys Acta 490:534–538
44. Mossing MC, Record MT Jr (1985) Thermodynamic origins of specificity in the lac repressor-operator interaction. Adaptability in the recognition of mutant operator sites. J Mol Biol 186:295–305
45. Royer CA, Weber G, Daly TJ, Matthews KS (1986) Dissociation of the lactose repressor protein tetramer using high hydrostatic pressure. Biochemistry 25:8308–8315
46. Royer CA, Chakerian AE, Matthews KS (1990) Macromolecular binding equilibria in the lac repressor system: studies using high-pressure fluorescence spectroscopy. Biochemistry 29:4959–4966
47. Gunsalus RP, Yanofsky C (1980) Nucleotide sequence and expression of *Escherichia coli* trpR, the structural gene for the trp aporepressor. Proc Natl Acad Sci U S A 77:7117–7121
48. Klig LS, Carey J, Yanofsky C (1988) Trp repressor interactions with the trp aroH and trpR operators. Comparison of repressor binding in vitro and repression in vivo. J Mol Biol 202:769–777
49. Rose JK, Yanofsky C (1974) Interaction of the operator of the tryptophan operon with repressor. Proc Natl Acad Sci U S A 71:3134–3138
50. Kelley RL, Yanofsky C (1982) Trp aporepressor production is controlled by autogenous regulation and inefficient translation. Proc Natl Acad Sci U S A 79:3120–3124
51. Fernando T, Royer C (1992) Role of protein–protein interactions in the regulation of transcription by trp repressor investigated by fluorescence spectroscopy. Biochemistry 31:3429–3441
52. Guest CR, Hochstrasser RA, Dupuy CG, Allen DJ, Benkovic SJ, Millar DP (1991) Interaction of DNA with the Klenow fragment of DNA polymerase I studied by time-resolved fluorescence spectroscopy. Biochemistry 30:8759–8770
53. Heyduk T, Lee JC (1990) Application of fluorescence energy transfer and polarization to monitor *Escherichia coli* cAMP receptor protein and lac promoter interaction. Proc Natl Acad Sci U S A 87:1744–1748
54. LeTilly V, Royer CA (1993) Fluorescence anisotropy assays implicate protein–protein interactions in regulating trp repressor DNA binding. Biochemistry 32:7753–7758
55. Otwinowski Z, Schevitz RW, Zhang RG, Lawson CL, Joachimiak A, Marmorstein RQ, Luisi BF, Sigler PB (1988) Crystal structure of trp repressor/operator complex at atomic resolution. Nature 335:321–329

56. Martin KS, Royer CA, Howard KP, Carey J, Liu YC, Matthews K, Heyduk E, Lee JC (1994) Electrostatic forces contribute to interactions between trp repressor dimers. Biophys J 66:1167–1173
57. Carey J, Combatti N, Lewis DE, Lawson CL (1993) Cocrystals of *Escherichia coli* trp repressor bound to an alternative operator DNA sequence. J Mol Biol 234:496–498
58. Grillo AO, Brown MP, Royer CA (1999) Probing the physical basis for trp repressor-operator recognition. J Mol Biol 287:539–554
59. Reedstrom RJ, Brown MP, Grillo A, Roen D, Royer CA (1997) Affinity and specificity of trp repressor-DNA interactions studied with fluorescent oligonucleotides. J Mol Biol 273:572–585
60. Grillo AO, Royer CA (2000) The basis for the super-repressor phenotypes of the AV77 and EK18 mutants of trp repressor. J Mol Biol 295:17–28
61. Kelley RL, Yanofsky C (1985) Mutational studies with the trp repressor of *Escherichia coli* support the helix-turn-helix model of repressor recognition of operator DNA. Proc Natl Acad Sci U S A 82:483–487
62. Reedstrom RJ, Royer CA (1995) Evidence for coupling of folding and function in trp repressor: physical characterization of the superrepressor mutant AV77. J Mol Biol 253:266–276
63. Billas I, Moras D (2013) Allosteric controls of nuclear receptor function in the regulation of transcription. J Mol Biol 425:2317–2329
64. Bain DL, Heneghan AF, Connaghan-Jones KD, Miura MT (2007) Nuclear receptor structure: implications for function. Annu Rev Physiol 69:201–220
65. Connaghan-Jones KD, Bain DL (2009) Using thermodynamics to understand progesterone receptor function: method and theory. Methods Enzymol 455:41–70
66. Boyer M, Poujol N, Margeat E, Royer CA (2000) Quantitative characterization of the interaction between purified human estrogen receptor alpha and DNA using fluorescence anisotropy. Nucleic Acids Res 28:2494–2502
67. Ozers MS, Hill JJ, Ervin K, Wood JR, Nardulli AM, Royer CA, Gorski J (1997) Equilibrium binding of estrogen receptor with DNA using fluorescence anisotropy. J Biol Chem 272:30405–30411
68. Poujol N, Margeat E, Baud S, Royer CA (2003) RAR antagonists diminish the level of DNA binding by the RAR/RXR heterodimer. Biochemistry 42:4918–4925
69. Szatkowski OM, Hill JJ, Ervin K, Royer CA, Gorski J (2001) The dissociation rate of estrogen receptor alpha from the consensus estrogen response element. Mol Cell Endocrinol 175:101–109
70. Bourdoncle A, Labesse G, Margueron R, Castet A, Cavailles V, Royer CA (2005) The nuclear receptor coactivator PGC-1alpha exhibits modes of interaction with the estrogen receptor distinct from those of SRC-1. J Mol Biol 347:921–934
71. le MA, Teyssier C, Erb C, Grimaldi M, Alvarez S, de Lera AR, Balaguer P, Gronemeyer H, Royer CA, Germain P, Bourguet W (2010) A unique secondary-structure switch controls constitutive gene repression by retinoic acid receptor. Nat Struct Mol Biol 17:801–807
72. Margeat E, Poujol N, Boulahtouf A, Chen Y, Muller JD, Gratton E, Cavailles V, Royer CA (2001) The human estrogen receptor alpha dimer binds a single SRC-1 coactivator molecule with an affinity dictated by agonist structure. J Mol Biol 306:433–442
73. Margeat E, Bourdoncle A, Margueron R, Poujol N, Cavailles V, Royer C (2003) Ligands differentially modulate the protein interactions of the human estrogen receptors alpha and beta. J Mol Biol 326:77–92
74. Nahoum V, Perez E, Germain P, Rodriguez-Barrios F, Manzo F, Kammerer S, Lemaire G, Hirsch O, Royer CA, Gronemeyer H, de Lera AR, Bourguet W (2007) Modulators of the structural dynamics of the retinoid X receptor to reveal receptor function. Proc Natl Acad Sci U S A 104:17323–17328
75. Pogenberg V, Guichou JF, Vivat-Hannah V, Kammerer S, Perez E, Germain P, de Lera AR, Gronemeyer H, Royer CA, Bourguet W (2005) Characterization of the interaction between

retinoic acid receptor/retinoid X receptor (RAR/RXR) heterodimers and transcriptional coactivators through structural and fluorescence anisotropy studies. J Biol Chem 280:1625–1633
76. Kallenberger BC, Love JD, Chatterjee VK, Schwabe JW (2003) A dynamic mechanism of nuclear receptor activation and its perturbation in a human disease. Nat Struct Biol 10:136–140
77. Savatier J, Jalaguier S, Ferguson ML, Cavailles V, Royer CA (2010) Estrogen receptor interactions and dynamics monitored in live cells by fluorescence cross-correlation spectroscopy. Biochemistry 49:772–781
78. Chiaruttini C, Milet M, Springer M (1996) A long-range RNA-RNA interaction forms a pseudoknot required for translational control of the IF3-L35-L20 ribosomal protein operon in *Escherichia coli*. EMBO J 15:4402–4413
79. Chiaruttini C, Milet M, de SM, Springer M (1996) Translational coupling in the *Escherichia coli* operon encoding translation initiation factor IF3 and ribosomal proteins L20 and L35. Biochimie 78:555–567
80. Guillier M, Allemand F, Raibaud S, Dardel F, Springer M, Chiaruttini C (2002) Translational feedback regulation of the gene for L35 in *Escherichia coli* requires binding of ribosomal protein L20 to two sites in its leader mRNA: a possible case of ribosomal RNA-messenger RNA molecular mimicry. RNA 8:878–889
81. Guillier M, Allemand F, Dardel F, Royer CA, Springer M, Chiaruttini C (2005) Double molecular mimicry in *Escherichia coli*: binding of ribosomal protein L20 to its two sites in mRNA is similar to its binding to 23S rRNA. Mol Microbiol 56:1441–1456
82. Raibaud S, Lebars I, Guillier M, Chiaruttini C, Bontems F, Rak A, Garber M, Allemand F, Springer M, Dardel F (2002) NMR structure of bacterial ribosomal protein l20: implications for ribosome assembly and translational control. J Mol Biol 323:143–151
83. Magde D, Elson EL, Webb WW (1974) Fluorescence correlation spectroscopy. II. An experimental realization. Biopolymers 13:29–61
84. Bacia K, Haustein E, Schwille P (2014) Fluorescence correlation spectroscopy: principles and applications. Cold Spring Harb Protoc 2014:709–725
85. Allemand F, Haentjens J, Chiaruttini C, Royer C, Springer M (2007) *Escherichia coli* ribosomal protein L20 binds as a single monomer to its own mRNA bearing two potential binding sites. Nucleic Acids Res 35:3016–3031
86. Doan T, Aymerich S (2003) Regulation of the central glycolytic genes in *Bacillus subtilis*: binding of the repressor CggR to its single DNA target sequence is modulated by fructose-1,6-bisphosphate. Mol Microbiol 47:1709–1721
87. Fillinger S, Boschi-Muller S, Azza S, Dervyn E, Branlant G, Aymerich S (2000) Two glyceraldehyde-3-phosphate dehydrogenases with opposite physiological roles in a nonphotosynthetic bacterium. J Biol Chem 275:14031–14037
88. Servant P, Le CD, Aymerich S (2005) CcpN (YqzB), a novel regulator for CcpA-independent catabolite repression of *Bacillus subtilis* gluconeogenic genes. Mol Microbiol 55:1435–1451
89. Zorrilla S, Ortega A, Chaix D, Alfonso C, Rivas G, Aymerich S, Lillo MP, Declerck N, Royer CA (2008) Characterization of the control catabolite protein of gluconeogenic genes repressor by fluorescence cross-correlation spectroscopy and other biophysical approaches. Biophys J 95:4403–4415
90. Zorrilla S, Chaix D, Ortega A, Alfonso C, Doan T, Margeat E, Rivas G, Aymerich S, Declerck N, Royer CA (2007) Fructose-1,6-bisphosphate acts both as an inducer and as a structural cofactor of the central glycolytic genes repressor (CggR). Biochemistry 46:14996–15008
91. Zorrilla S, Doan T, Alfonso C, Margeat E, Ortega A, Rivas G, Aymerich S, Royer CA, Declerck N (2007) Inducer-modulated cooperative binding of the tetrameric CggR repressor to operator DNA. Biophys J 92:3215–3227
92. Chaix D, Ferguson ML, Atmanene C, Van DA, Sanglier-Cianferani S, Royer CA, Declerck N (2010) Physical basis of the inducer-dependent cooperativity of the central glycolytic genes repressor/DNA complex. Nucleic Acids Res 38:5944–5957

93. Digman MA, Dalal R, Horwitz AF, Gratton E (2008) Mapping the number of molecules and brightness in the laser scanning microscope. Biophys J 94:2320–2332
94. Ferguson ML, Le CD, Jules M, Aymerich S, Declerck N, Royer CA (2011) Absolute quantification of gene expression in individual bacterial cells using two-photon fluctuation microscopy. Anal Biochem 419:250–259